

III-4

Surface,
Interface and
Thin Films

BL2B

An Optimization Study for Multi-Alkali Photocathode as the Ultimate Electron Source

M. Kuriki¹, Y. Seimiya¹, T. Konomi², M. Katoh² and R. Inagaki³

¹Graduate school of Advanced Science of Matter, Hiroshima University, Higashi-hiroshima, 739-8530, Japan

²UVSOR Facility, Institute for Molecular Science, Okazaki 444-8585, Japan

³Graduate School of Engineering, Nagoya University, Nagoya 464-8603, Japan

Multi-alkali photocathode, CsK₂Sb is the strongest candidate as the ultimate photocathode for high-brightness electron accelerator. Recently, advanced accelerator projects based on the linear accelerator (Linac) have been proposed and some of them, e.g. X-ray FEL, are already in operation. To realize a high brightness beam with Linac, the electron source is one of the key components, because the beam brightness normalized with its energy is kept during the acceleration over Linac. From the view point of electron source, a small emittance and large current beam from a small spot size has to be generated. As the cathode requirements, not only the small emittance, but also high quantum efficiency (QE) and high robustness are required. In addition, if the visible light laser instead of UV laser which is commonly used for metal cathode is applicable, it relaxes the technical requirements for the laser. CsK₂Sb cathode fulfills these requirements; high QE as high as more than 10%, driven by a green laser, and high robustness [1]. CsK₂Sb is then suitable for the high brightness Linac application. On the other hand, CsK₂Sb cathode is made with evaporation in a vacuum chamber as a thin film in order of several 10s nm. The cathode activity is lost by air exposure. The evaporation condition to maximize the cathode performance is not established and material property is not well understood. The aim of our study is to understand the cathode performance from the material science point of view.

We made the multi-alkali evaporation chamber which is capable to form the thin film in an extreme vacuum environment. The thin-film cathode is made on a substrate fixed on a sample holder. The pressure of the chamber was 5.0×10^{-8} Pa.

Figure 1 shows an example of CsK₂Sb evaporation. The horizontal axis shows time in minutes and $t=0$ gives the start of the evaporation. On boron doped p-type Si substrate (100), Sb, K, and Cs were evaporated in this order. The thickness was measured with a quartz monitor. QE was measured with 405 nm laser. It was more than 8%.

Figure 2 shows UPS spectrum for CsK₂Sb. By comparing Sb peaks[2][3], Sb 4d peaks split into 5. The valence band peaks are enhanced. Peak at 18 and 10 eV are consistent with K 3p[4] and Cs 5p[5], respectively, but need more careful investigation for the identification.

As the summary, we successfully took UPS spectra for (multi) alkali cathode evaporated on Si substrate.

To identify the optimized evaporation condition for the thin film cathode, UPS spectra of the cathode evaporated with various different conditions should be taken. UPS spectral change during the cathode degradation should give curious information about the process.

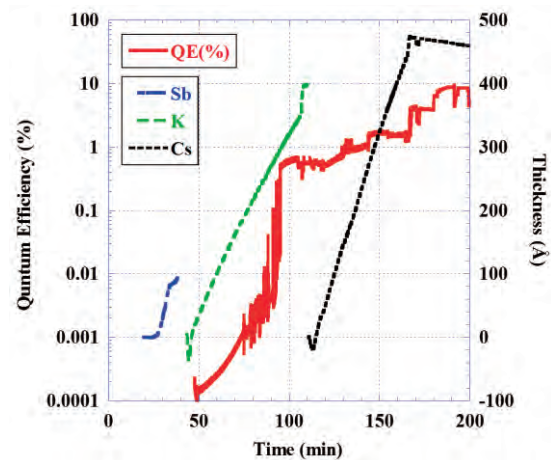


Fig. 1. An example of evaporation of CsK₂Sb. The right and left vertical axes show thickness (Angstrom) and QE (405nm) in %.

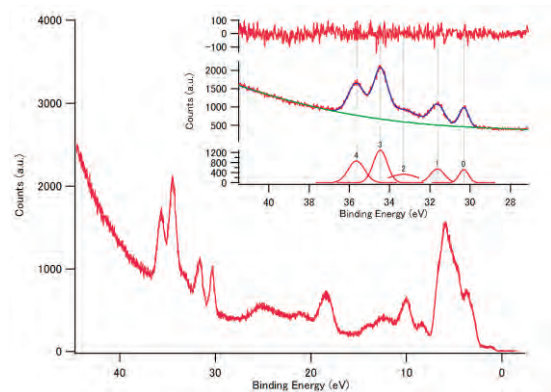


Fig. 2. CsK₂Sb UPS spectrum as a function of binding energy.

- [1] B. Dunham *et al.*, Appl. Phys. Lett. **102** (2013) 034105.
- [2] M. Scrocco *et al.*, J. Electron Spectrosc. Relat. Phenom. **50** (1990) 171.
- [3] G. E. Franklin *et al.*, Phys. Rev. B **45** (1992) 3426.
- [4] H. H. Weitering *et al.*, Phys. Rev. B **48** (1993) 8119.
- [5] A. N. Belsky *et al.*, J. Electron Spectrosc. Relat. Phenom. **80** (1996) 109.

BL2B

Electronic Structure of Chlorophyll-a Investigated by Photoelectron Spectroscopy and Photoelectron Yield Spectroscopy

Y. Takeda¹, H. Ezawa², T. Miyauchi¹, H. Kinjo¹, K. R. Koswattage³,
Y. Nakayama¹ and H. Ishi^{1,3}

¹Advanced Integration Science, Chiba University, Chiba 263-8522, Japan

²Department of Engineering, Chiba University, Chiba 263-8522, Japan

³Center for Frontier Science, Chiba University, Chiba 263-8522, Japan

Observing the electronic structures of bio-molecules in their living environment is indispensable to elucidate their functionalities. Especially understanding how photosystem of plants realizes energy conversion in high efficiency is an important factor for the development of artificial photosynthesis. In photosystem, photon energy is converted to electron energy by photoexcitation reaction of Chlorophyll-a (Chl-a) aggregation. In addition, in actual systems, Chl-a is surrounded by solvent. In water-rich acetone-water binary solvent, Chl-a exists predominantly as oligomer, which have been utilized as artificial model of Chl-a in vivo [1]. For general materials, photoelectron spectroscopy (PES) is a powerful and widely used technique to examine their electronic structures. However, PES needs vacuum environment and its application to bio-related systems has been much limited. In this study, we tried to observe the electronic structure of Chlorophyll-a (Chl-a) with the techniques.

Chl-a powder was bought from Wako Pure Chemical Industries and was used as purchased. Sample of UPS was spin-coated film which was deposited acetone solution of chlorophyll a on ITO. For PYS, Chl-a powder was dissolved in water-rich (83.3 vol%) acetone-water binary solution (0.7 mM), in which almost all Chl-a molecules are known to exist as oligomers, which have been utilized as an artificial in vivo model of RC [1]

Figure 1 a) shows UPS results by Synchrotron radiation at BL2B. Blue line is estimated DOS and red line is the observed spectra. The observed spectral feature is consistent with calculated DOS. Weak sample-charge-up seems to slightly induce the spectral broadening. Moreover, we measured Low Energy UPS and the determined that the ionization energy of Chl-a film was 5.0eV. In addition, gap state was observed above HOMO as shown in Fig. 1 b). The spectra HOMO state may spread due to the variation of molecular packing. Figure 2 shows PYS spectra of Chl-a solution and a film which was measured after drying up of the solution. The ionization energies of Chl-a in the solution and solid phase were determined to be $I_1 = 4.9_5$ eV and $I_s = 4.9_3$ eV, respectively. Its ionization energy in the gas phase had been reported to be $I_g = 6.1$ eV [2] which was collaborated by DFT calculation. Hence the polarization energies P_+ of Chl-a in the solvent is

estimated to be 1.2 eV by the formula: $P_+ = I_g - I_1$. Interestingly this value is 0.5 eV smaller than a literature value of P_+ (=1.7eV [3]) for a water molecule induced by adjacent H₂O molecules. This suggest that large molecules like Chl-a reduce polarization energy by water.

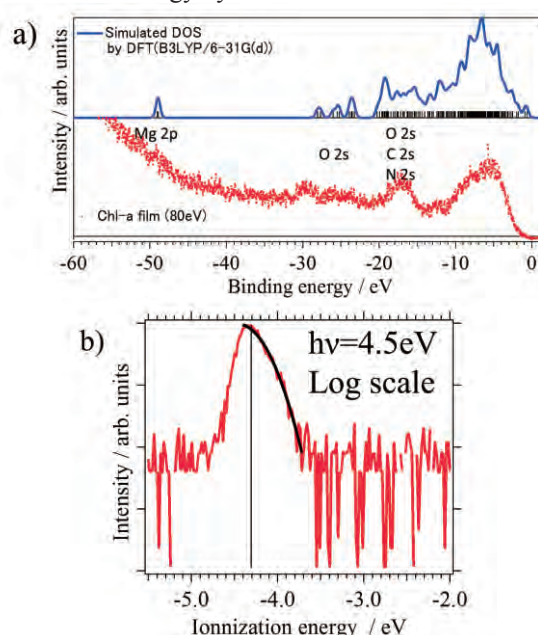


Fig. 1. UPS spectrum of the Chl-a film
a)UPS by Synchrotron radiation, b)Low Energy UPS.

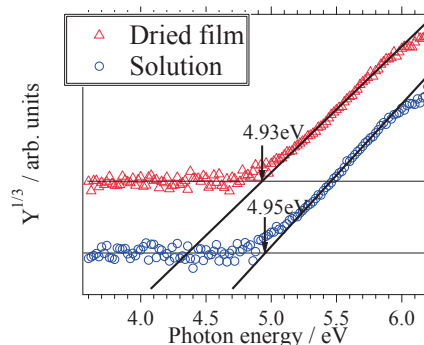


Fig. 2. PYS spectra of Chl-a in the solution and solid phases.

[1] Agostiano *et al.*, BBA BIOENER. **936** (1988) 171.

[2] Y. Nakato *et al.*, Chem. Soc. Jpn. **47** (1974) 3001.

[3] M. Faubel *et al.*, J. Chem. Phys. **106** (1997) 9013.

BL3U

Cobalt-Borate Oxygen Evolution Catalyst Studied by Electrochemical XAFS Technique Using Soft X-Ray

Y. Mitsutomi¹, M. Yoshida^{1,2}, T. Mineo¹, M. Kawamura¹, M. Nagasaka³, H. Yuzawa³,
N. Kosugi³ and H. Kondoh¹

¹Department of Chemistry, Keio University, Yokohama 223-8522, Japan

²Cooperative Research Fellow, Catalysis Research Center, Hokkaido University, Sapporo 001-0021, Japan

³Institute for Molecular Science, Okazaki 444-8585, Japan

Photoelectrochemical water splitting using solar energy is an attractive candidate to produce hydrogen gas from water. This system consists of two half reactions of hydrogen and oxygen evolutions. Among of them, the rate of oxygen evolution is generally slower than that of hydrogen evolution. Thus, the development of efficient oxygen evolution catalyst has been required toward highly active energy conversion system. Recently, a cobalt-borate electrodeposited from a dilute Co^{2+} solution in a borate-buffered electrolyte (Co-B_i) was reported to function as an efficient electrocatalyst for oxygen evolution reaction [1]. The structural information was investigated by X-ray pair distribution function (PDF), which indicates that Co-B_i catalyst is formed by coherent domains consisting of 3–4 nm cobaltate clusters with up to three layers [1]. However, the correlation between structure and activity is still unclear. Therefore, in this study, the Co-B_i catalyst was investigated by *in-situ* O K-edge XAFS measurements under potential control conditions.

Electrochemical XAFS measurements with transmission mode using soft X-rays were performed at BL3U in the UVSOR Synchrotron, according to the previous work [2]. A home-made electrochemical cell was used with Au/Cr/SiC thin film substrates as working electrodes, a Pt mesh counter electrode, and a Ag/AgCl (saturated KCl) reference electrode. Co-B_i catalyst was prepared on the Au/Cr/SiC working electrode at 1.0 V in 0.1 M K-B_i electrolyte containing 0.5 mM $\text{Co}(\text{NO}_3)_2$.

Figure 1 shows the linear sweep voltammograms of bare and Co-B_i-modified Au electrodes in 0.1 M K-B_i electrolyte. The current density of oxygen evolution reaction for Co-B_i-modified electrode was higher than that for bare Au electrode, which exhibits that Co-B_i can function as an efficient oxygen evolution catalyst. Figure 2 shows the O K-edge XAFS spectra for Co-B_i catalyst at 1.0 V in a 0.1 M K-B_i. Two absorption peaks were observed at ca. 529.3 eV and 530.9 eV for Co-B_i sample. Empirically, the O K-edge absorption peak position shifts to lower energies with increasing the formal oxidation state. Thus, the absorption peak at ca. 529.3 eV is likely to be attributed to a high-valent cobalt species. Further investigation is in progress in order to reveal the relationship between production of high-valent cobalt species and oxygen evolution activity.

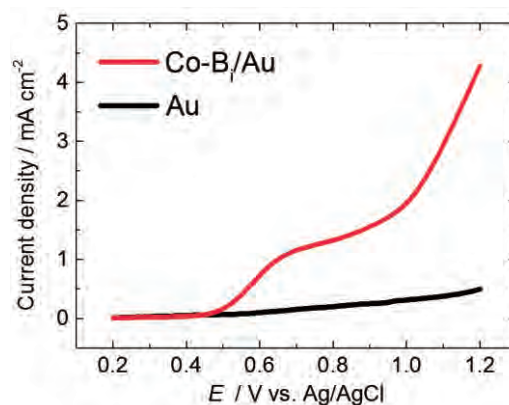


Fig. 1. Linear sweep voltammograms of the bare and Co-B_i-modified Au electrodes in 0.1 M K-B_i (pH 9.2) electrolyte at 100 mV/s.

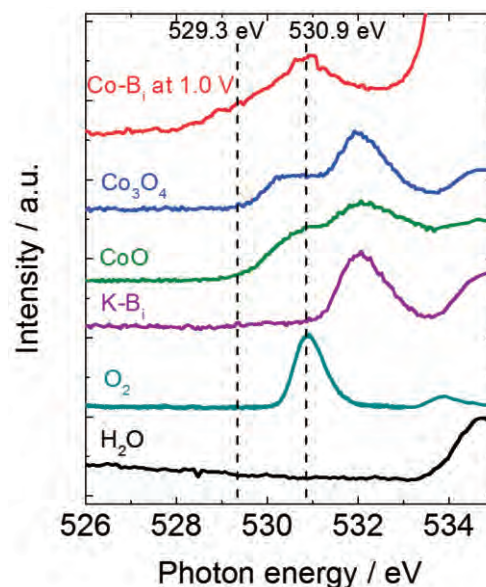


Fig. 2. O K-edge XAFS spectra of Co-B_i catalyst on the Au/Cr/SiC electrode at 1.0 V in 0.1 M K-B_i. The spectra of Co_3O_4 , CoO, K-B_i, O_2 , and H_2O are shown as reference samples.

[1] D. G. Nocera *et al.*, *J. Am. Chem. Soc.* **135** (2013) 6403.

[2] M. Nagasaka *et al.*, *J. Electron. Spectrosc. Relat. Phenom.* **177** (2010) 130., *J. Phys. Chem. C* **117** (2013) 16343., *Rev. Sci. Instrum.* **85** (2014) 104105.

BL4U

STXM Analysis of Adsorbent for Effective Recovery of Radioactive Elements

Y. Sano¹, S. Watanabe¹, H. Matsuura² and A. Nezu²

¹Japan Atomic Energy Agency (JAEA), Tokai-mura 319-1194, Japan

²Research Laboratory for Nuclear Reactors, Tokyo Institute of Technology, Tokyo 152-8550, Japan

Spent nuclear fuels generated from nuclear power plants contain U and Pu which can be reused, and several long-lived radioactive elements. It will be quite important for effective utilization of energy and environmental loading reduction to process the spent fuel adequately. JAEA has been developing the selective recovery process of radioactive elements, which uses adsorbents of SiO₂ supports coated with styrene-divinylbenzene copolymer (SiO₂-P) and extractants on its surface [1]. Our recent work shows that the separation and recovery abilities of adsorbent, i.e. adsorption/elution behavior of radioactive elements, in this process are strongly dependent on the condition of its surface in which polymer and extractants are impregnated [2]. In this study, some information about the adsorbent surface, such as uniformity of extractants and SiO₂/polymer/extractants interaction, were investigated by scanning transmission X-ray microscope (STXM).

Some adsorbents with different crosslinking degree of polymer (CDP) were synthesized and octyl (phenyl)-N, N-diisobutylcarbonoylmethylphosphine oxide (CMPO) was impregnated as an extractant by the flowsheet reported by Wei et al. [3]. The average diameter and pore size of the synthesized adsorbents were 50μm and 50nm, respectively (Fig.1). These adsorbents were sliced to 1~3μm in thickness by focused ion beam (FIB), and were supplied to STXM analysis.

Figures 2 and 3 show the STXM image of adsorbent surface and the change of O-NEXAFS spectra with CDP at 530eV (O-K edge), respectively. The intensity of pre-edge peak at 532eV increased with CDP at any positions in the adsorbent. The impregnation of CMPO into the adsorbent showed no significant effect on these results.

The appearance of pre-edge peak at 530eV in O-NEXAFS spectra with increasing CDP indicates the some interactions between SiO₂ and the polymer or/and the capture of some kinds of molecules, such as H₂O, by the polymer. These will give some interpretation of our previous experiment, in which it was more difficult to elute adsorbed metal ions from the adsorbent with higher CDP [2]. To obtain more detailed information about the adsorbent surface, STXM analyses at 300eV (C-K edge) and 189eV (P-K edge) will be carried out. It should be further required for effective recovery of radioactive elements to evaluate and compare the STXM data and adsorption/elution behavior using several kinds of adsorbents with different pore sizes and extractants.

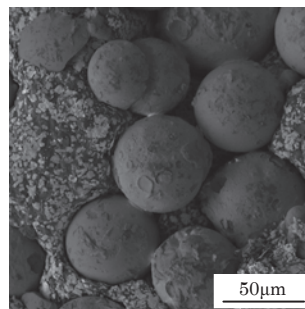


Fig. 1. Photo of the SiO₂-P adsorbents (CDP: 10%).

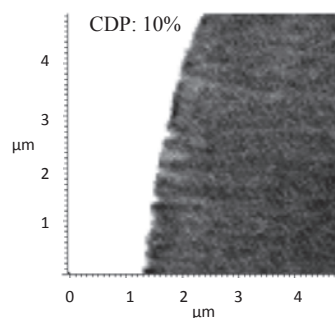


Fig. 2. STXM image of the surface of the SiO₂-P adsorbent at 530eV (O-K edge).

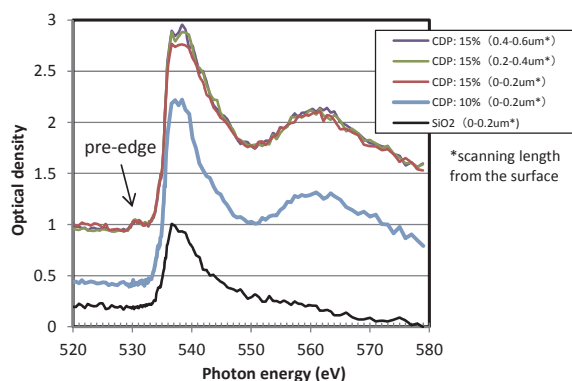


Fig. 3. Change of O-NEXAFS spectra with CDP at 530eV (O-K edge)

[1] Y. Koma *et al.*, Proc. OECD Nuclear Energy Agency 11th Information Exchange Meeting on Actinide and Fission Product Partitioning and Transmutation, San Francisco, USA, November 1-4, (2010) IV-4.

[2] S. Watanabe *et al.*, Procedia Chemistry 7 (2012) 411.

[3] Y. Wei, M. Kumagai and Y. Takashima, Nucl. Technol. 132 (2000) 413.

BL4B

XMCD Study on Magnetic Multilayer of CoNi₂ on W(110)

 T. Yasue¹, M. Suzuki¹, T. Nakagawa², K. Takagi³, T. Yokoyama³ and T. Koshikawa¹
¹Fundamental Electronics Research Institute, Osaka Electro-Communication University,
Neyagawa 572-8530, Japan

²Department of Molecular and Material Sciences, Kyusyu University, Fukuoka 816-8580, Japan

³Institute for Molecular Science, Okazaki 444-8585, Japan

Co/Ni₂ multilayer shows the perpendicular magnetic anisotropy (PMA) and hence is attracted much attention as a candidate for the spintronics device based on the current induced domain wall motion. We have investigated the dynamic behavior of emerging PMA during the multilayer growth process on W(110) by a high-brightness and highly spin polarized low energy electron microscopy (SPLEEM) [1]. In the beginning of the growth below 3 Co/Ni₂ pairs, the perpendicular magnetization appears during Ni deposition, while the magnetization becomes in-plane by Co deposition. PMA becomes stable after 4 pairs even after Co deposition. In order to understand the behavior, XMCD measurements were performed at BL4B in the present work.

Ni L_{2,3} and Co L_{2,3} XMCD spectra were taken at the incident angle of X-ray of 60° (GI) and 0° (NI) with applying the external high magnetic field enough to saturate the magnetization. The magnetic field was parallel to the X-ray direction. The spin magnetic moments m_s and the orbital magnetic moments m_o of Ni and Co were derived from the measured XMCD spectra using the sum rules.

The white line intensities of Ni and Co L_{2,3} absorption spectra were almost constant over different multilayer repetitions examined. The white line intensity is proportional to the number of 3d holes, so that the charge transfer between Ni, Co and the substrate W could be negligible. On the contrary, XMCD spectra strongly depend on the multilayer repetition. This indicates that the spin and orbital moments vary in the multilayer stacking sequence. Figure 1 shows m_o/m_s ratio of Ni taken at NI (red) and GI (blue). At NI configuration, the m_o/m_s ratio increases with coverage, and decreases at GI. This result clearly indicates that the orbital moment of Ni plays an important role for the perpendicular magnetization at higher coverage. Figure 2 shows the spin (squares) and orbital moments (circles) of Ni (top) and Co (bottom). The parallel (blue) and perpendicular (red) components are separated for the orbital moment. Both spin and orbital moments of Co do not show clear coverage dependence, while those of Ni increase with coverage up to 3 pairs and reach to the constant value above 4 pairs. The perpendicular orbital moment of Ni becomes more dominant with increasing coverage. Therefore it is concluded that PMA of the Co/Ni₂ multilayer is mainly induced by the perpendicular orbital moment of Ni.

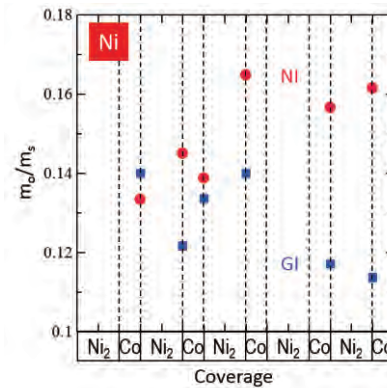


Fig. 1. Ratio of the orbital moment to the spin moment of Ni. Red circles are taken at NI and blue squares at GI.

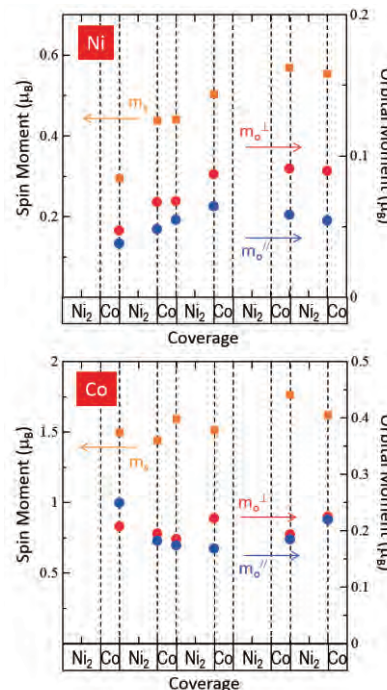


Fig. 2. Spin and orbital magnetic moments of Ni (top) and Co (bottom) obtained by XMCD measurements.

[1] M. Suzuki, K. Kudo, K. Kojima, T. Yasue, N. Akutsu, W. A. Diño, H. Kasai, E. Bauer and T. Koshikawa, J. Phys.: Condens. Matter **25** (2013) 406001.

BL4B

XMCD Study of Anisotropic Magnetism of Fe/W(112)

K. Yamaguchi, T. Kawashima, S. Mizuno and T. Nakagawa

Department of Molecular and Material Sciences, Kyushu University, Kasuga 816-8580, Japan

Ordered atoms on surfaces have highly anisotropic structures which is not available for the bulk materials. Such strained or low dimensional structures bring anisotropic electronic structures, resulting in interesting magnetic properties. One-dimensional structures are successfully prepared on stepped surfaces and shows intriguing magnetic properties, which has attracted much attention [1,2]. On the other hand, other works on bcc(112), highly anisotropic surfaces, are also interesting due to its furrow structure (Fig.1), which would exhibit high magnetic anisotropy. However few investigation of magnetic overlayers on bcc(112) have been examined so far [3], and its magnetic properties are unknown. We have prepared Fe quasi-chain structure on W(112) surface and investigated its magnetic properties.

X-ray magnetic circular dichroism (XMCD) measurements were done at BL4B using high field and low temperature end station. All the measurements were performed *in situ* under the vacuum of 1×10^{-10} Torr.

Figure 1 shows anisotropic Fe quasi chain structure on W(112), as determined by tensor low energy diffraction (LEED) analysis (Fig.1 (a)), and visualized by STM (Fig.1(b)). Fe atoms occupy the furrow of W(112), and forms 1×1 structure, irrespective of the large size mismatch between Fe and W ($\sim 10\%$), in accordance with other Fe monolayer structures on W(111), W(110), and W(100) surfaces.

Figure 2 shows Fe-L XAS for 0.6 ML Fe/W(112) and its XMCD. Figure 3 shows magnetization curves (M - H curves) for 0.6 ML Fe/W(112), which was measured by monitoring Fe L_3 XAS intensity. The M - H curve along the $[11\bar{1}]$ direction shows hysteresis with the large coercivity of 3.7 T, while the M - H curves along the $[112]$, surface normal, and the $[1\bar{1}0]$ directions do not show hysteresis and do not saturate even at $H = 5$ T. This M - H curve measurement reveals that the magnetization easy axis is along the $[11\bar{1}]$ direction, parallel to the quasi Fe chains and that the magnetic anisotropy energy is 0.6 meV/Fe atom.

In summary, XMCD study reveals that Fe/W(112) exhibits the large magnetic anisotropy and coercivity as expected from its anisotropic structure.

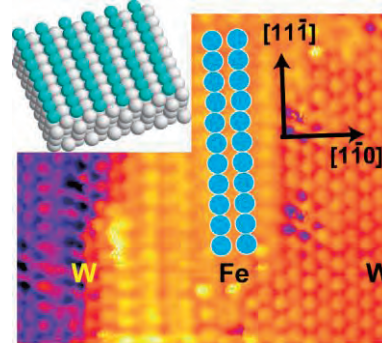


Fig. 1. A structure model of Fe(1 ML)/W(112) determined by tensor LEED and its atomically resolved STM image.

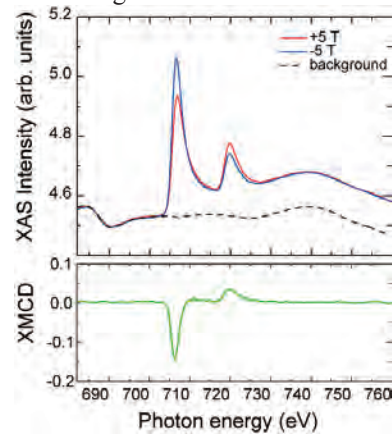


Fig. 2. XAS and XMCD spectra for Fe(0.6 ML)/W(112) for $H = \pm 5$ T along the $[11\bar{1}]$ direction with the background contribution from W(112) clean surface.

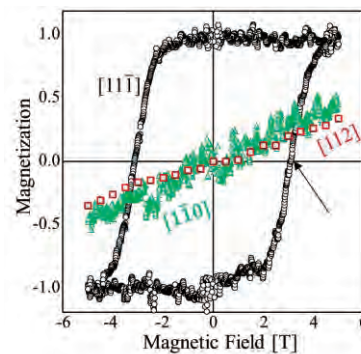


Fig. 3. Magnetization curves for Fe(0.6 ML)/W(112) taken along three different directions.

- [1] M. Pratzner *et al.*, Phys. Rev. Lett. **87** (2001) 127201.
- [2] P. Gambardella *et al.*, Nature **416** (2002) 301.
- [3] J. Kołaczekiewicz and E. Bauer, Surf. Sci. **144** (1984) 495.
- [4] T. Nakagawa *et al.*, Phys. Rev. B **86** (2012) 144418.

BL4B

X-Ray Magnetic Circular Dichroism Study of Mn- and Fe-Phthalocyanine Molecules Self-Assembled on the Si(111)-($\sqrt{7}\times\sqrt{3}$)-In Surface

T. Uchihashi and S. Yoshizawa

International Center for Materials Nanoarchitectonics (MANA), National Institute for Materials Science, Tsukuba 305-0044, Japan

Recently, atomic-layer superconductors on silicon surface (surface reconstructions) were investigated by electron transport measurement and scanning tunneling microscopy. The superconductivity of this class of atomically thin materials can be tuned by adsorption of molecules due to its high surface sensitivity. In this work, we studied the magnetic properties of Mn-Phthalocyanine (Pc) and FePc self-assembled on the Si(111)-($\sqrt{7}\times\sqrt{3}$)-In surface reconstruction [referred to as ($\sqrt{7}\times\sqrt{3}$)-In], which is made of atomic indium layers on a clean silicon surface [1,2]. Since the ($\sqrt{7}\times\sqrt{3}$)-In surface exhibits superconducting phase transition at 3 K, interesting competition effects between superconductivity and magnetism are expected to occur in this system.

X-ray absorption spectroscopy (XAS) and X-ray magnetic circular dichroism (XMCD) measurements [3,4] were taken to detect the magnetic properties of the MnPc and FePc. The experiment was performed in the ultrahigh vacuum XMCD system with a superconducting magnet, which was set at the UVSOR beam line BL4B in the Institute for Molecular Science. First, preparation of the ($\sqrt{7}\times\sqrt{3}$)-In surface was confirmed by low energy electron diffraction (LEED) (Fig. 1). MnPc was then evaporated to a monolayer level. Parallel molecular adsorption geometry on the surface was confirmed from the XAS measurement of N K-edge. Similar results were obtained for or FePc on the ($\sqrt{7}\times\sqrt{3}$)-In surface. XMCD spectra were determined from the difference between the XAS spectra taken at $T=5\text{K}$ and $B = \pm 5\text{T}$.

We found clear XMCD signal for both MnPc and FePc molecules, which showed that the spins of Mn and Fe atoms coordinated at the Pc molecules were retained even when they are adsorbed onto the ($\sqrt{7}\times\sqrt{3}$)-In surface (Fig. 2). Detailed analysis of the XMCD data using the sum rule gives the following results. MnPc (1ML, $\theta=55^\circ$): $\langle S_{\text{eff}} \rangle = 0.94 \pm 0.18 \mu_B$, $\langle L \rangle = 0.61 \pm 0.08 \mu_B$, FePc (1ML, $\theta=55^\circ$): $\langle S_{\text{eff}} \rangle = 0.50 \pm 0.23 \mu_B$, $\langle L \rangle = 0.31 \pm 0.12 \mu_B$. Therefore, it is concluded that MnPc and FePc have about one and half spins, respectively, on adsorption. The observed orbital magnetic moments were also found to be relatively large in both cases. These magnetic moments should influence the superconductivity of the ($\sqrt{7}\times\sqrt{3}$)-In surface at low temperatures.

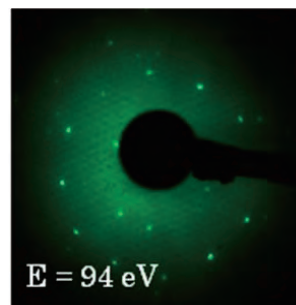


Fig. 1. LEED patterns of the ($\sqrt{7}\times\sqrt{3}$)-In sample before evaporation of Pc molecules.

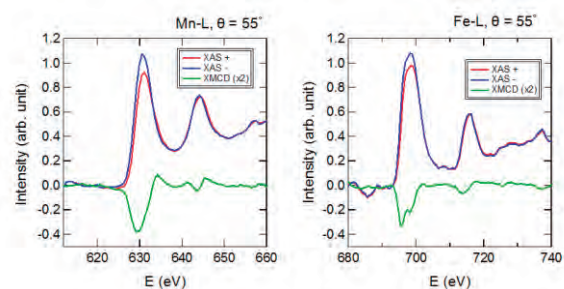


Fig. 2. XAS and XMCD spectra taken for Mn-L edge (MnPc) and Fe-L edge (FePc) at $T = 5\text{K}$, $B = \pm 5\text{T}$, and $\theta=55^\circ$. The coverage of the molecule is 1ML for both cases.

- [1] T. Uchihashi *et al.*, Phys. Rev. Lett. **107** (2011) 207001.
- [2] S. Yoshizawa *et al.*, Phys. Rev. Lett. **113** (2014) 247004.
- [3] S. Stepanow *et al.*, Phys. Rev. B **82** (2010) 014405.
- [4] K. Eguchi *et al.*, J. Phys. Chem. C **118** (2014) 17633.

BL4B

Magnetic Properties of Ordered Iron Nitride Monatomic Layer

T. Miyamachi¹, Y. Takahashi¹, Y. Takagi^{2,3}, M. Uozumi^{2,3}, T. Yokoyama^{2,3} and F. Komori¹

¹*Institute for Solid State Physics, University of Tokyo, Kashiwa 277-8581, Japan*

²*Department of Materials Molecular Science, Institute for Molecular Science, Okazaki 444-8585, Japan*

³*Department of Structural Molecular Science, The Graduate University for Advanced Studies (SOKENDAI), Okazaki 444-8585, Japan*

Iron nitrides, especially in iron-rich phases as represented by Fe_{16}N_2 [1], or F_4N [2], are of great interest for the field of materials science due to their extraordinarily large magnetic anisotropy and room-temperature ferromagnetism. Towards practical applications, deep understanding of their magnetic properties in the form of thin films and extremely of a monatomic layer is required. For this purpose, we fabricated well-ordered iron nitride monatomic layer (Fe_2N layer) on a $\text{Cu}(001)$ substrate and performed x-ray magnetic circular dichroism (XMCD) measurements at BL4B in UVSOR by total electron yield mode.

The Fe_2N layer was fabricated by three processes, i.e., (1) ionic bombardment of N^+ onto a clean $\text{Cu}(001)$ surface with a beam energy of 500 eV, (2) Fe deposition onto N^+ -bombarded $\text{Cu}(001)$ at room temperature, and (3) subsequent annealing up to ~ 700 K. The high-quality surface of the Fe_2N layer with a $p4gm(2 \times 2)$ reconstruction was confirmed before XMCD measurements by scanning tunneling microscopy and low energy electron diffraction.

Figure 1(a) displays XMCD spectra obtained at $B = 5$ T and $T = 7.2$ K in the in-plane ($\theta = 55^\circ$) and the out-of-plane ($\theta = 0^\circ$) geometries by detecting $\mu_+ - \mu_-$, where μ_+ (μ_-) denote the x-ray adsorption spectrum (XAS) with the photon helicity parallel (antiparallel) to the sample magnetization. θ is defined as the angle between the sample normal and the incident x-ray. We find that the XMCD intensity in the in-plane geometry is greater than that in the out-of-plane geometry, which indicates the magnetic easy axis of the Fe_2N layer is towards in-plane direction.

The easy magnetization direction of the Fe_2N layer is clearly recognized by the magnetization curves. Figure 1(b) displays the magnetization curves obtained in the in-plane and out-of-plane geometries. The data points represent the $\text{Fe } L_3$ intensity as a function of applied magnetic field. A steplike magnetization curve with a clear hysteresis loop near $B = 0$ T [see inset of Fig. 1(b)] is observed in the in-plane geometry, while the magnetization curve in the out-of-plane geometry can be fit rather well by a simple Langevin function. Furthermore, the intensity of the in-plane remanent XMCD signal in Fig. 1 (c) monotonously decreases with increasing temperature, but the reduction was only by $\sim 20\%$ when temperature is increased from 7.2 to 41 K. These facts would reveal that the Fe_2N layer is ferromagnetic with a strong in-plane magnetic anisotropy, in good

agreement with a recent study [3].

Detailed analyses of the XMCD spectra and the temperature dependence of the remanent XMCD signal give further information on the magnetic moments and the Curie temperature of the Fe_2N layer. In future work, combined XMCD with surface analysis techniques, the correlation between magnetism and surface quality of the Fe_2N layer will be also discussed.

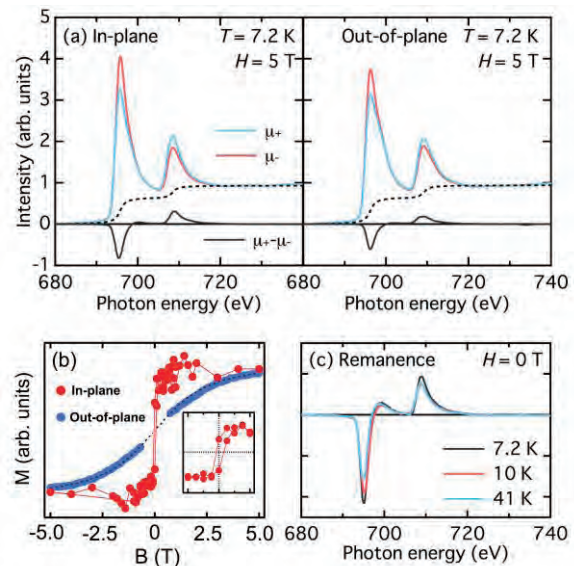


Fig. 1. (a) XAS and XMCD spectra obtained at $B = 5$ T and $T = 7.2$ K in the in-plane and out-of-plane geometries. (b) Magnetization curves obtained at $T = 7.2$ K in the in-plane and out-of-plane geometries. (c) Remanent XMCD spectra obtained at $T = 7.2, 10,$ and 41 K.

[1] K. H. Jack, Proc. R. Soc. London, Ser. A **208** (1951) 200.

[2] J. M. Gallego *et al.*, Phys. Rev. B **70** (2004) 115417.

[3] Y. Takagi *et al.*, Phys. Rev. B **81** (2010) 035422.

BL4B

Magnetism of Oxygen Covered Fe Monolayer on Mo(110)

T. Nakagawa¹, Y. Higuchi¹, K. Yamaguchi¹, S. Mizuno¹, Y. Takagi² and T. Yokoyama²

¹Department of Molecular and Material Sciences, Kyushu University, Kasuga 816-8580, Japan

²Institute for Molecular Science, Okazaki 444-8585, Japan

Iron oxides have a variety of structures, which show intriguing magnetic ordering such as antiferromagnetism in FeO, ferrimagnetism in Fe₃O₄. Thin film iron oxides have been studied since they are important for basic research and solid devices, but few studies have been devoted to understand their magnetic properties of the single layer unit [1].

Experiments were done at x-ray magnetic circular dichroism (XMCD) endstation with a superconducting magnet ($H \sim 6$ T). Fe was deposited on Mo(110) which was cleaned by repeated cycles of oxidation at 1500 K and high temperature annealing up to 2200 K. Subsequently the monolayer Fe film was exposed to oxygen with the crystal temperature kept at room temperature. We found three Fe oxide structures, namely $p(3 \times 2)$, $p(5 \times 1)$, and quasi-FeO(111), which is in good agreement with the previously reported structures for O/Fe/W(110)[1]. The structural consistency is plausible since both of W and Mo substrates have similar crystal and electronic structures.

Figure 1(a) shows Fe L edge XAS spectra for Fe/Mo(110) with different exposures to oxygen. Here 1 L corresponds to 1×10^{-6} Torr s. With increasing the exposure, the white line intensity gradually increases, indicating the increase of Fe 3d hole. The L_2 peak around $h\nu = 720$ eV shows clear difference due to the oxidation. The spectrum with the exposure of 150 L shows a splitting at L_2 with 718 and 721 eV, while the spectra for the Fe films exposed up to 17 L does not show the splitting. According to the previous XAS result [2], the oxygen covered Fe at 150 L is FeO.

Oxygen adsorption on Fe/Mo(110) drastically modifies the magnetization. Figure 1(b) shows XMCD spectra for various oxygen adsorption. The application of the conventional sum rule gives the effective magnetic moment of $2.0 \mu_B$ for the clean Fe monolayer, which is the sum of the orbital and effective spin moment including the dipole term. When Fe is exposed to 0.2 L oxygen, corresponding to the appearance of the first super structure, $p(3 \times 2)$, the XMCD intensity decreases, resulting in $0.3 \mu_B$ of the magnetic moments. When the $p(3 \times 2)$ is completed, the magnetic moment is suppressed to $0.2 \mu_B$. With further expose to oxygen, the magnetic moment slightly increases to $0.4 \mu_B$ at 17 L, but it is almost zero at 150 L.

In conclusion, the oxygen adsorption on monolayer Fe drastically deactivates ferromagnetism, and the resulting structures are antiferromagnetic or paramagnetic structures.

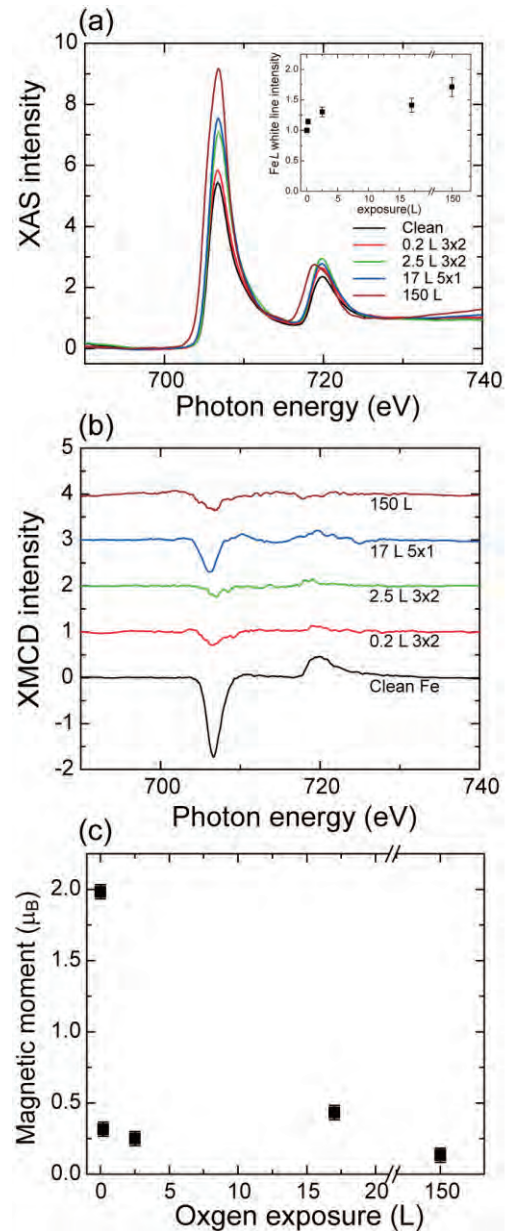


Fig. 1. (a) XAS spectra for Fe films exposed to 0, 0.2, 2.5, 17, and 150 L oxygen taken at $T_s = 5$ K with the light incidence normal to the surface. The inset is the Fe L edge white line intensity. (b) The same as (a), but XMCD spectra taken at $H = \pm 5$ T. (c) Magnetic moment obtained from the sum rule analysis.

[1] K. Feindl *et al.*, Surf. Sci. **617** (2013) 183.

[2] P. S. Miedema and F. M. F. de Groot, J. Electron Spectrosc. Relat. Phenom. **187** (2013) 32.

BL5B

Characterization of Amorphous Chalcogenide Thin Films by Vacuum Ultraviolet Transmission Spectroscopy

K. Hayashi

Department of Electrical, Electronic and Computer Engineering, Gifu University, Gifu 501-1193, Japan

Amorphous chalcogenide semiconductor materials are very expected as a potential material for optoelectronic devices. Because, in these materials are very sensitive to the light, and show a variety of photoinduced phenomena [1-3]. For device applications, it is necessary to sufficiently understand the fundamental properties of these materials. Although a large number of studies have been done on the photoinduced phenomena of these materials, little is known about the details of these mechanisms. These phenomena were studied by exciting outer core electrons with the irradiation of light with the energy corresponding to the optical bandgap or sub-bandgap. The interest has been attracted for the change of the optical properties in the energy region of the visible light. We are interesting for the changes of the optical properties in the higher energy region. To obtain a wide knowledge of the photoinduced phenomena, it is necessary to investigate to the photoinduced effects on wide energy region. In previous reports, we reported the photoinduced change at the VUV transmission spectra of amorphous thin films [4]. In this report, we investigated the photoinduced effects on the as-deposited film by VUV transmission spectroscopy. We also report on the annealing effects at glass transition temperature.

Samples used for the measurement of the VUV transmission spectra were amorphous chalcogenide ($a\text{-As}_2\text{Se}_3$ and $a\text{-As}_2\text{S}_3$) semiconductor thin films prepared onto aluminum thin films by conventional evaporation technique. Typical thickness of the samples and the aluminum films were around 180nm and 100nm respectively. The aluminum film of the thickness of 100 nm was also used in order to eliminate the higher order light from the monochromator in the VUV region. The measurements were carried out at room temperature at the BL5B beam line of the UVSOR facility of the Institute for Molecular Science. And the spectrum was measured by using the silicon photodiode as a detector. Two pinholes of 1.5mm in a diameter were inserted between the monochromator and sample to remove stray light. The intensity of the VUV light was monitored by measuring the TPEY of a gold mesh. The positions of the core levels for the samples were calibrated by referencing to the 2p core level absorption peak of the aluminum film.

Figure 1 shows the VUV transmission spectra of $a\text{-As}_2\text{Se}_3$ film in each state. Two main absorption peaks were observed in this wavelength region. One absorption peak around 22nm corresponds to the 3d

core level of Se atom. Another absorption peak around 28nm corresponds to the 3d core level of As atom. As shown in the figure, the photoinduced changes are observed on the transmission spectra before and after the irradiation of the bandgap (BG) light. We think that those changes are related to the local structures of the amorphous network. The annealing effect on the film after the irradiation by the BG light did not appear clearly as a change in spectrum shape. More detailed experiments are necessary to clarify the origin of the photoinduced changes of the VUV transmission spectra.

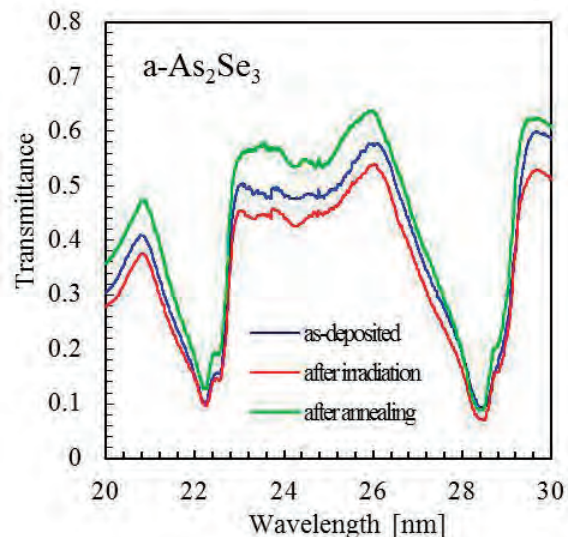


Fig. 1. VUV transmission spectra of $a\text{-As}_2\text{Se}_3$ thin film in each state.

- [1] K. Tanaka, *Rev. Solid State Sci.* **4** (1990) 641.
- [2] K. Shimakawa, A. Kolobov and S. R. Elliott, *Adv. Phys.* **44** (1995) 475.
- [3] K. Tanaka, *Encyclopedia of Nanoscience and Nanotechnology* **7** (2004) 629.
- [4] K. Hayashi, *UVSOR Activity Report 2013* **41** (2014) 140.

BL6U

Phase-Dependent Electronic Structure of Superstructure Monolayer of Hexa-*peri*-Hexabenzocoronene on Au(111)

H. Yamane and N. Kosugi

Department of Photo-Molecular Science, Institute for Molecular Science, Okazaki 444-8585, Japan

The intermolecular interaction is a key issue in molecular electronic properties. It has been reported that hexa-*peri*-hexabenzocoronene (HBC) on Au(111) forms various ordering phases in the monolayer, e.g., $(5 \times 5)R0^\circ$ “R0 phase”, $(\sqrt{27} \times \sqrt{27})R30^\circ$ “R30 phase”, and their mixed phase, depending on the preparation condition [1,2]. In the present work at BL6U, in order to examine the lateral intermolecular interaction in flat-lying molecular layers, we investigated the electronic structure of the R0 and R30 phases of HBC on Au(111), which was realized by controlling the substrate temperature during the thin-film growth.

Figure 1 shows the low-energy electron diffraction (LEED) image, the surface Brillouin zone (SBZ), and the energy-*versus*-momentum [$E(\mathbf{k})$] map of the R0 and R30 phases of the HBC monolayer on Au(111) at 15 K, obtained from angle-resolved photoemission spectroscopy (ARPES). In the R0 phase, the highest occupied molecular orbital (HOMO, H_0) disperses in a narrow width by 20 meV only along the k_{TK} direction, and the HOMO-1 (H_1) disperses by 25 meV only along the k_{TM} direction, which is more evident in the selected energy distribution curve (EDC) in Fig. 1. The opposite trend was observed in the R30 phase; that is, the HOMO disperses by 20 meV along the k_{TM} direction, and the HOMO-1 disperses by 25 meV along the k_{TK} direction. The observed dispersion periodicity is dependent on the high symmetric points of $\bar{\Gamma}$, \bar{K}' , and \bar{M}' in SBZ of the HBC superstructure; therefore, the observed π -band dispersion rationally arises from the intermolecular interaction.

The lateral intermolecular π -band dispersion in organic monolayers has been reported for strongly chemisorbed interfaces with the 0.2-0.3 eV dispersion width [3,4], which is 10 times larger than the present dispersion. Such large dispersions are caused by the substrate-mediated intermolecular interaction due to the strong orbital hybridization and the highly ordered structure at the interface [3,4]. In the present case, the interfacial electronic coupling is weak because of the observation of the vibrationally-resolved HOMO line shape, as indicated by the downed arrow. In addition, we observed no evidence for the interfacial charge transfer. These evidences are the indication of the weak interaction at the interface. Furthermore, the substrate-mediated π -band dispersion should be observed along the underlying metal-atom array [3,4]. Since the present π -band dispersion is dependent not on the substrate SBZ but on the molecular SBZ, the observed π -band dispersion might be introduced by a lateral intermolecular interaction.

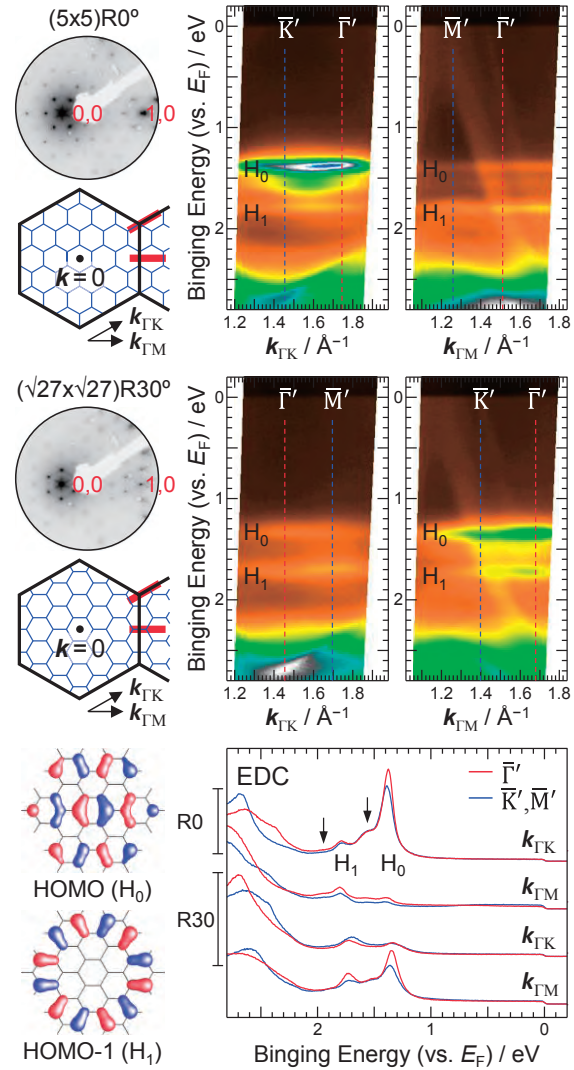


Fig. 1. LEED, SBZ [thick-black hexagon for Au(111) and thin-blue hexagon for HBC], wherein the red line indicates the scanned region in ARPES, the $E(\mathbf{k})$ map, and the EDCs at the high symmetric point of the superstructure monolayer of HBC/Au(111) with the $(5 \times 5)R0^\circ$ and $(\sqrt{27} \times \sqrt{27})R30^\circ$ phases at 15 K. The LCAO patterns of the HOMO and HOMO-1 of HBC are also shown.

- [1] D. Kasemann *et al.*, *Langmuir* **25** (2009) 12569.
- [2] C. Wagner *et al.*, *Phys. Rev. B* **81** (2010) 035423, and references therein.
- [3] H. Yamane *et al.*, *Phys. Rev. B* **76** (2007) 165436; *J. Electron Spectrosc. Rel. Phenom.* **174** (2009) 28.
- [4] M. Wießner *et al.*, *Nat. Commun.* **4** (2013) 1514; *Phys. Rev. B* **88** (2013) 075437.

BL6U

Formation of Delocalized π Band and Interface State in Superstructure Monolayer of Coronene on Au(111)

H. Yamane and N. Kosugi

Department of Photo-Molecular Science, Institute for Molecular Science, Okazaki 444-8585, Japan

Polycyclic aromatic hydrocarbons have attracted attention again as a fragment of graphene. In the present work, by using angle-resolved photo emission spectroscopy (ARPES), we have studied the electronic structure of a (4×4) superstructure monolayer of coronene on Au(111).

The experiment was performed at the in-vacuum undulator beamline BL6U. The cleanliness of the Au(111) surface was confirmed by the low-energy electron diffraction (LEED) and the Shockley state in ARPES, as obtained from the repeated cycles of the Ar^+ sputtering and the subsequent annealing at 700 K. The total energy resolution in ARPES was 13 meV.

Figures 1 shows (a) a LEED image at 15 K and (b) the corresponding surface Brillouin zone (SBZ) of the coronene monolayer on Au(111). The LEED image shows the (4×4) superstructure with respect to the Au(111) hexagonal lattice, as reported in Ref. [1]. The ARPES spectra were measured by considering the high symmetric points of $\bar{\Gamma}'$, \bar{K}' , and \bar{M}' in the molecular SBZ [blue hexagon in Fig. 1(b)].

The energy-*vs*-momentum $E(\mathbf{k})$ relation map of the coronene (4×4) /Au(111) along the $\bar{\Gamma}'$ - \bar{K}' and $\bar{\Gamma}'$ - \bar{M}' (\mathbf{k}_{TK} and \mathbf{k}_{TM}) directions, obtained from ARPES, is shown in Figs. 1(c) and 1(d), respectively. The highest occupied molecular orbital (HOMO, π) derived peak of coronene is observed at the binding energy (E_b) of 1.6 eV. Although no direct intermolecular π - π overlap exist in the coronene monolayer, the HOMO peak shows a quite weak

lateral band dispersion by 30 meV at $\bar{\Gamma}'$ - \bar{K}' and by 15 meV at $\bar{\Gamma}'$ - \bar{M}' . The observed dispersion is larger than that for the (5×5) hexa-*peri*-hexabenzocoronene (HBC) superstructure monolayer on Au(111) [2]. This difference is explained by the smaller molecular unit cell and the shorter inter-molecular spacing of the coronene monolayer than those of the HBC monolayer. The observed π -band dispersion is ascribed to the lateral intermolecular interaction in flat-lying aromatic hydrocarbons.

On the other hand, the interface-specific electronic states are observed around the $\bar{\Gamma}'$ point as labeled IS_1 , IS_2 , and IS_3 in Figs. 1(c) and 1(d), which show the relatively large dispersion with the evidence for the spin-orbit splitting. These interface states may originate from the backfolded Shockley- and Tamm-type electronic states of the Au(111) surface at the $\bar{\Gamma}$ and \bar{M} points, respectively, induced by the superstructure. Note that, the observed dispersions are modified from the original Shockley and Tamm states in terms of the effective mass, the Rashba parameter, and so on. Such modifications might be introduced by the Pauli repulsion of surface electrons due to adsorbates and by the scattering due to the superstructure lattice.

[1] C. Seidel *et al.*, Phys. Rev. B **64** (2001) 195418.

[2] H. Yamane *et al.*, a separate page in this volume, UVSOR Activity Report 2014.

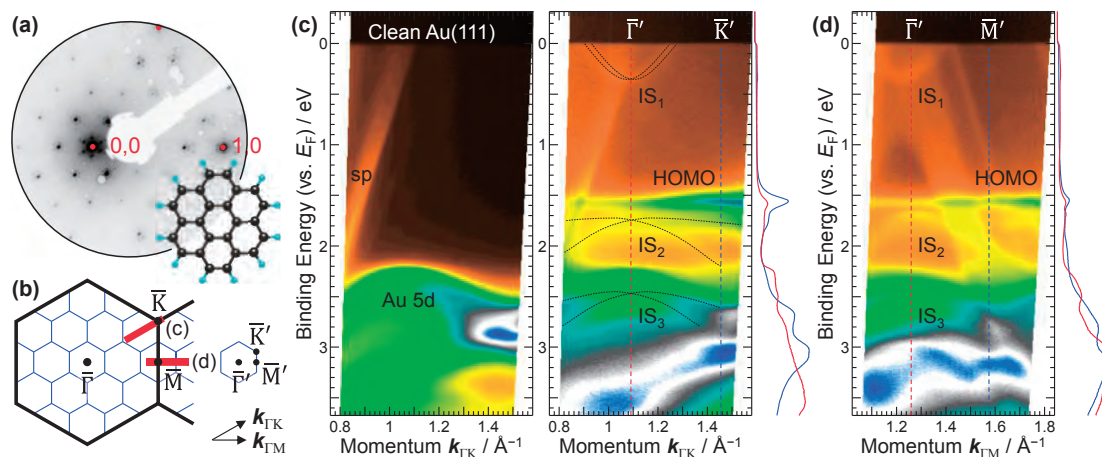


Fig. 1. (a) LEED of the coronene (4×4) /Au(111) at 15 K, wherein the red dot indicates the substrate's spot. The molecular structure of coronene is also shown. (b) SBZ of the Au(111) (black) and the coronene (4×4) /Au(111) (blue). The red line indicates the scanned region in ARPES. (c,d) The $E(\mathbf{k})$ maps of the clean Au(111) and the coronene (4×4) /Au(111) at 15 K along the \mathbf{k}_{TK} and \mathbf{k}_{TM} directions. The energy distribution curves at $\mathbf{k}_{\text{TK}} = 1.08 \text{ \AA}^{-1}$ ($\bar{\Gamma}'$), 1.44 \AA^{-1} (\bar{K}') and $\mathbf{k}_{\text{TM}} = 1.25 \text{ \AA}^{-1}$ ($\bar{\Gamma}'$), 1.56 \AA^{-1} (\bar{M}') are also shown.

BL6U

Manybody Interactions in Rb-Doped Graphene

W. J. Shin^{1,2}, S. H. Ryu^{1,2}, H. Yamane³, N. Kosugi³, K. S. Kim^{1,2} and H. W. Yeom^{1,2}

¹Center for Artificial Low Dimensional Electronic Systems, Institute for Basic Science (IBS), 77 Cheongam-Ro, Pohang 790-784, Korea

²Department of Physics, Pohang University of Science and Technology, 77 Cheongam-Ro, Pohang 790-784, Korea

³Department of Photo-Molecular Science, Institute for Molecular Science, Okazaki 444-8585, Japan

Graphene has served as a prototypical model system for study of various low-dimensional physics [1]. It has rather simple lattice and electronic structures, and the energy scale of phonons, collective excitations of periodic atoms, is relatively large (up to ~200 meV), making it ideal to investigate the electron-phonon interaction and its interplay with electron correlations [2]. Angle-resolved photo emission spectroscopy (ARPES) is an ideal technique that can directly observe energy band dispersion of electrons. Also, ARPES is capable of probing not only a signature of electron-phonon interactions that appear as an abrupt slope change in band dispersion (kink) [2,3], but also electron correlations that lead to the multiple Dirac points. Indeed, high-resolution ARPES spectra from heavily doped graphene have shown such kink structures and band renormalizations [4,5].

In this work, we have measured a systematic evolution of graphene π bands as increasing the Rb density (Fig. 1). We found the phase separation of Rb dopants that the two distinct doping levels coexist at the moderate Rb density. This can be understood by the different degree of charge transfer between the scatter Rb atoms and Rb islands. From the kinked dispersion we could compare electron-phonon and electron-electron coupling constants, which turn out to be different from those for K atoms as dopants. This shows a different degree of screening (or dielectric constant of dopant islands) between Rb and K. We anticipate that this work would provide a meaningful step forward to understanding manybody correlations in heavily-doped graphene as well as to searching for superconductivity in graphene with a relatively high transition temperature.

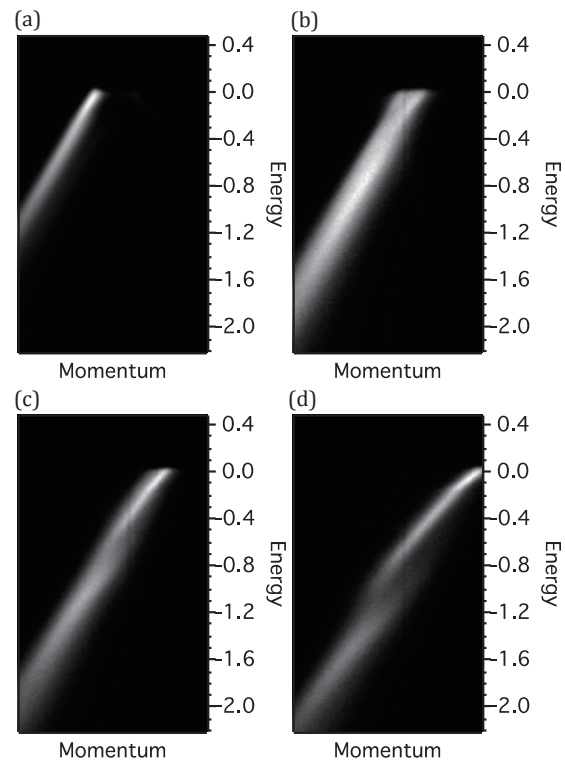


Fig. 1. Doping dependence of band dispersions of rubidium doped graphene.

- [1] H. Castro Neto *et al.*, Review of Modern Physics **81** (2009) 109.
- [2] C. S. Leem *et al.*, Physical Review Letters **100** (2008) 016802.
- [3] A. Damascelli *et al.*, Review of Modern Physics **75** (2003) 473.
- [4] A. Bostwick *et al.*, Nature Physics **3** (2007) 36.
- [5] S. Y. Zhou *et al.*, Physical Review B **78** (2008) 193404.

BL6U

Surface Coordination Chemistry to Control the Charge Transfer at Organic/Metal Interface: SnCl₂Pc on Ag(111)

S. Kera^{1,2}, K. Yonezawa², T. Tago², F. Bussolotti¹, H. Yamane¹,
N. Kosugi¹ and K. K. Okudaira²

¹Department of Photomolecular Science, Institute of Molecular Science, Okazaki, 444-8585, Japan

²Department of Nanomaterial Science, Graduate School of Advanced Integration Science, Chiba University, Chiba 263-8522, Japan

For more than two decades molecular adsorbates on metal surfaces represent a very active field of research in surface and interface science. Fundamental understanding the basic physical properties is a key issue for tuning the geometric and electronic structure at the interfaces, hence to improve and control the organic device performance. To understand the mechanism of charge transfer (CT) at organic/metal interfaces, the binding energy of frontier orbitals (HOMO and LUMO) and the adsorption height of the molecules on the metal are critical parameters.

Using coordination chemistry we introduce “spacers” which change the contact distance to the surface, and investigate the consequences for geometric (adsorption height, molecular bending, etc.) and electronic structure (amount of CT). In contrast to planer phthalocyanines (Pc), dichlorotin Pc (SnCl₂Pc) is an n-type semiconductor and its conductivity is 1–3 orders larger than most of the other Pcs. In this study, we performed ARUPS and XPS for SnCl₂Pc films prepared on Ag(111). Since the size of the SnCl₂ group is large, the molecule is considered to be non-planar, but there is no permanent dipole.

The experiments were conducted at BL6U. The clean surface was obtained by the repeated cycles of Ar⁺ sputtering and annealing. After preparing the monolayer film (0.4nm) on the Ag(111) at room temperature, valence band (VB) and secondary cut-off (SECO) was measured at 45eV, then each core levels are scanned for C1s, N1s, Cl2p, and Sn4d. The same measurements are repeated for the annealed monolayer film (633K for 3h). We evaluated the photoelectron angular distribution of HOMO and concluded the flat-lying orientation both for as-grown and annealed films (not shown).

Figure 1 shows the Cl2p XPS spectra of SnCl₂Pc/Ag(111) before and after the annealing. For the as-grown film, spin-orbit splitting of Cl2p is detected in different binding energies for upper- (towards the vacuum) and lower-side (to the substrate) of Cl atoms. However the peaks disappear totally for the annealed film. Considering energy shifts in other core levels, the chemical structure may change to SnPc by removing the Cl atoms.

Figure 2 shows the angle-integrated UPS for VB and SECO regions. Regardless of Cl atoms, clearly

the gap state due to the CT from the metal to the LUMO state is observed as for other metal-Pcs on Ag(111) [1]. By detaching the Cl atoms, HOMO shifts to high energy side to show a very similar spectrum to SnPc/Ag(111) [1]. The work function is reduced by 0.2eV upon annealing, which might be caused by differences in total CT amount and/or push-back effects induced by rearrangement of the adsorption height.

It is an open question if this chemisorption with CT involves the anchored Cl atom via an expanded LUMO orbital, or whether basically the indole groups bond to the surface due to a strongly distorted or tilted geometry. A geometrical study including a precise determination of adsorption height will give a clear answer for these.

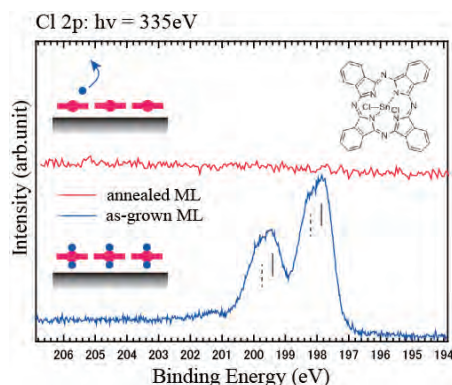


Fig. 1. Cl2p XPS spectra for SnCl₂Pc/Ag(111) taken at 297K for as-grown and annealed film.

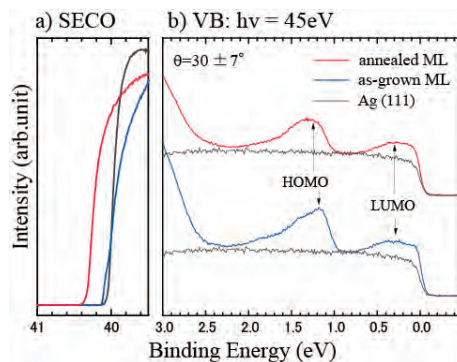


Fig. 2. a) SECO and b) VB for SnCl₂Pc/Ag(111) taken at 297K for as-grown and annealed film. The spectra for the clean substrate are also shown.

[1] M. Häming *et al.*, Phys. Rev. B **82** (2010) 235432.

BL7U

Electronic Structure of a MnSe/Bi₂Se₃ Ultrathin Film Heterostructure

T. Hirahara¹, T. Kubo², A. Takayama², T. Hajiri³, M. Matsunami³,
K. Tanaka³ and S. Hasegawa²

¹Department of Physics, Tokyo Institute of Technology, Tokyo 152-8551, Japan

²Department of Physics, University of Tokyo, Tokyo 113-0033, Japan

³UVSOR Facility, Institute for Molecular Science, Okazaki 444-8585, Japan

Topological insulators (TI) are extensively studied recently due to its peculiar properties [1]. The Dirac-cone surface states of TI are protected by time-reversal symmetry (TRS) and backscattering among these surface states is prohibited. But when TRS is broken by application of a magnetic field or incorporating magnetic materials, a gap opening in the Dirac cone is expected and an intriguing phase called the quantum anomalous Hall state can be realized [2]. This phase is expected to show even more exotic phenomena such as the topological magnetoelectric effect. To realize such state, two types of sample fabrication techniques have been employed up to now: (1) magnetic doping while growing the single crystal or thin film of TI [3], and (2) magnetic impurity deposition on the surface of TI [4]. While method (1) was successful and showed evidence of the TRS violation, no one has succeeded using method (2), which should be a more direct way to examine the interaction between the topological surface states and magnetism.

In the present work, we have attempted an alternative approach to break the TRS in TI: making a heterostructure of TI and magnetic insulators (MI) and making use of the magnetic proximity effect at the interface. For this purpose, we have fabricated a heterostructure of MnSe (MI) and Bi₂Se₃ (TI) since the lattice mismatch between the two materials is relatively small (~6%). MnSe is a layered structure and is antiferromagnetic as a whole, but in each Mn layer, the spin is oriented in one direction (ferromagnetic within the layer and antiferromagnetic among the adjacent layers) [5]. Thus one can expect that the ferromagnetic Mn layer will break TRS of TI. Figures 1 (a) and (b) show the band dispersion of the surface states of Bi₂Se₃ and the 2BL MnSe/Bi₂Se₃ heterostructure. While the Dirac-cone surface states are massless in (a), one can find a clear gap of ~ 80 meV at the Dirac point in (b), meaning that it has turned into a massive Dirac cone. This result shows that our method is indeed a successful way to induce TRS breaking in TI surface states. Spin- and angle-resolved photoemission measurements will be performed to see the change of the spin-polarization of the Dirac cone upon the gap opening.

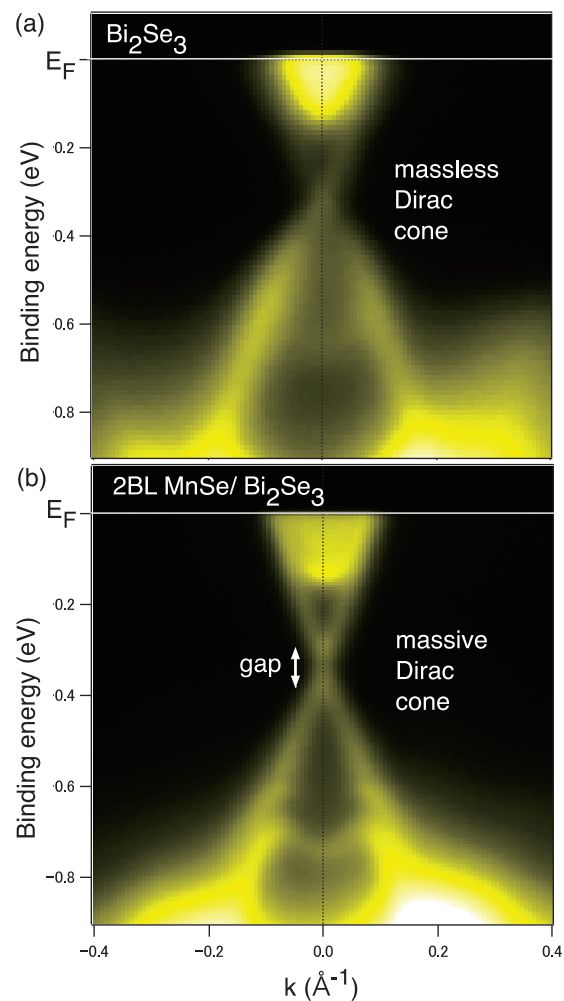


Fig. 1 The band dispersion of Bi₂Se₃ (a), and a heterostructure of MnSe/Bi₂Se₃, respectively measured at $h\nu = 21$ eV with p -polarization.

[1] M. Hasan and C. Kane, *Reviews of Modern Physics* **82** (2010) 3045.

[2] X.-L. Qi and S.-C. Zhang, *Reviews of Modern Physics* **83** (2011) 1057.

[3] For example, C. Z. Chang *et al.*, *Science* **340** (2013) 167.

[4] For example, M. Ye *et al.*, *Physical Review B* **85** (2012) 205317.

[5] R. J. Pollard *et al.*, *J. Phys. C: Solid State Phys.* **16** (1983) 345.

BL7U

Angle-Resolved Photoelectron Spectroscopy Study of One-Dimensional Electronic States on Bi/InSb(001)

Y. Ohtsubo^{1,2}, J. Kishi², K. Hagiwara², M. Matsunami³, K. Tanaka³ and S. Kimura^{1,2}

¹Graduate School of Frontier Biosciences, Osaka University, Suita 565-0871, Japan

²Department of Physics, Graduate School of Science, Osaka University, Toyonaka 560-0043, Japan

³UVSOR Facility, Institute for Molecular Science, Okazaki 444-8585, Japan

One-dimensional (1D) metals behave in completely different ways from ordinal 3D metals [1]. Tomonaga Luttinger liquid (TLL) is one of the most extensively studied phases as an example of the exotic 1D metals. It is theoretically predicted that TLL should exhibit exotic power-law scaling and spin-charge separation [2]. So far, various 1D systems with 1D structure were studied as candidates of TLL and only a few of them showed metallic states with power-law spectral features *e.g.* carbon nanotube [3] and Lithium purple bronze (LiPB) [4, 5].

On the surface of semiconductor, various self-assembled 1D atomic structures are known and they have been regarded as suitable systems to study 1D metallic states [1]. However, most of them do not behave as TLL at low temperature, because of 2D undulation of the surface states and/or metal-insulator transition driven by strong nesting. Up to now, the only system claimed as a surface TLL is the Au nanowire assembled on Ge(001) [6]. However, even on Au/Ge(001), the direction of conduction path and even the nature of TLL itself is still under debate.

In this project, we have performed angle-resolved photoelectron spectroscopy (ARPES) study on the surface 1D system Bi/InSb(001). Bi/InSb(001) is reported to form an 1D atomic structure with metallic electronic states [7] and hence the encouraging candidate of surface TLL. ARPES measurements were performed at the beamline BL7U of UVSOR-III. The InSb(001) substrate is cleaned by repeated cycles of sputtering and annealing and then Bi is evaporated from a home-made Knudsen cell. The sample preparation process was performed *in situ*.

Figure 1 (a) shows the Fermi surface of Bi/InSb(001) taken at room temperature. The Fermi surface clearly shows the 1D and metallic features of the surface electronic states of Bi/InSb(001). No k_z dispersion of the metallic state was observed with different photon energies (not shown here), indicating that it is the 1D surface state. The 1D state disperses along the 1D chain direction (the relationship between the surface periodicity and 1D atomic-chain direction has been already reported in Ref. [7]).

We examined the polarization dependence of the metallic 1D state. As shown in Fig. 1 (b) and (c), the surface state is observed only with *P*-polarized photons. Broad features below 0.6 eV come from bulk bands. The clear polarization dependence on the surface state indicates the even symmetry of the 1D

state with respect to the photon-incident plane.

Further analysis based on temperature dependence and spectral shape around the Fermi level is in progress in order to examine whether the 1D surface state on Bi/InSb(001) behaves as TLL or not.

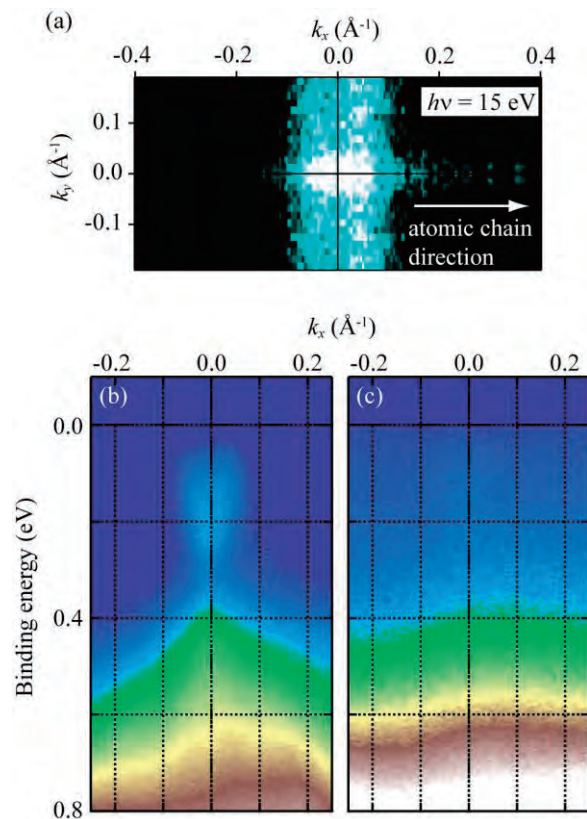


Fig. 1. The Fermi surface (a) and band dispersion (b, c) of the Bi/InSb(001) surface taken at $h\nu = 15$ eV. (b) and (c) are measured with *P*- and *S*- linearly polarized photons, respectively.

[1] M. Grioni *et al.*, J. Phys.: Condens. Matt. **21** (2009) 023201.

[2] S. Tomonaga, Prog. Theor. Phys. **5** (1950) 544.

[3] H. Ishii *et al.*, Nature **426** (2003) 540.

[4] F. Wang *et al.*, Phys Rev. Lett. **96** (2006) 196493.

[5] L. Dudy *et al.*, J. Phys.: Condens. Matt. **25** (2013) 014007.

[6] C. Blumenstein *et al.*, Nat. Phys. **7** (2011) 776.

[7] P. Laukkanen *et al.*, Phys. Rev. B **81** (2010) 035310.

BL7U

Formation of the Dirac Cone at the Γ -Point on the Epitaxial Graphene Sheet Observed by the Angle-Resolved Photoelectron Spectroscopy with the Low Energy Photon

S. Tanaka¹, T. Maruyama², M. Matsunami³ and K. Tanaka³¹*Institute of Scientific and Industrial Research, Osaka University, Ibaraki 567-004, Japan*²*Department of Materials Science and Engineering, Meijo University, Nagoya 468-8502, Japan*³*UVSOR Facility, Institute for Molecular Science, Okazaki 444-8585, Japan*

Graphene, a single-atomic-layer consisting of a carbon sp^2 -orbital-network, is one of the materials that have been most extensively studied these years. Here, for the first time, we report a peculiar behavior of the epitaxial single-layer graphene formed on the SiC crystal; a backfolding of the Brillouin zone which enables an observation of the characteristic Dirac cone at the Γ -point, which is located at the K-point in the normal Brillouin zone of the graphene.

The experiments were made at the BL-7U, UVSOR-III. The sample used was provided by the “Graphene Platform” inc, and cleaned by heating at 700C° in UHV. The sample was then moved to the experimental chamber and slowly cooled down to 13K for measuring the angle-resolved photoelectron spectra (ARPES) near the surface-normal direction as a function of the photon energy. Figure 1 shows volume and plane ($k_y=0$) maps of the ARPES intensity taken at $h\nu=10.8\text{eV}$ as functions of the momentum parallel to the graphene sheet and the electron binding energy. The feature in the ARPES spectra is absolutely agreed with the so called “Dirac cone”, which is consisting of linearly dispersed π -bands and most prominent characteristics of the graphene. The Dirac point is located 0.4 eV below the Fermi level, which indicates that a single-layer of the graphene is formed. This behavior is very surprising, since the Dirac cone of the graphene exists not at the Γ -point but at the K-point of the Brillouin zone, (separated by 1.7 \AA^{-1} from the Γ -point) which cannot be accessed with the ARPES technique below the photon energy of 15.4eV if the work function of 4.5eV is assumed. Since the defects or electron-phonon scattering cannot be a candidate considering the momentum and energy conservation rule, the most probable interpretation is the surface Umklapp process, in which the electron is diffracted from K to Γ due to the formation of the superstructure (e.g., $(\sqrt{3} \times \sqrt{3})R30^\circ$) formed on the graphene layer. As shown in Fig.2, this Dirac cone is only observed when the photon energy is near 11eV. This clearly indicates that the final state located 11eV above the Fermi level plays a key role for this observation. Thus, it seems reasonable the scattering occurs among the unoccupied bands located this energy region.

We found that the surface normal photoelectron emission due to the Dirac cone is extinguished when the sample is warmed to 50K. This behavior is similar

to the superstructure formation on the graphite surface, where the CDW transition was proposed[1], and similar transition may occur on the graphene surface and/or the step edge. However, this superstructure on the graphene surface is less stable than the graphite surface, and we could not find a definite condition for the observation of the Dirac cone, and more work is needed for a deeper understanding the physical nature of this surprising phenomenon.

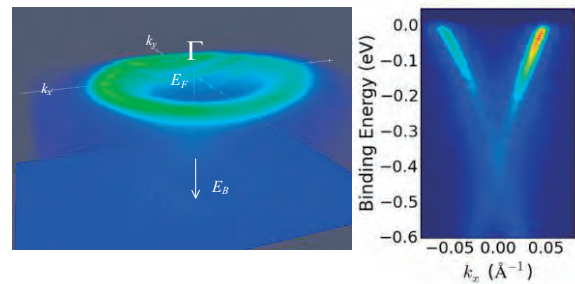


Fig. 1. ARPES results of epitaxial graphene on SiC (13K) near Fermi level at the Γ -point (surface normal) taken at $h\nu=10.8\text{eV}$.

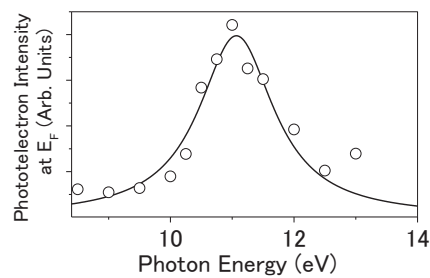


Fig. 2. Photoelectron intensity near the Fermi level in the ARPES spectra of graphene as a function of the excitation photon energy. The line is a Lorentzian curve centered at 11.1eV.

[1] S. Tanaka, M. Matsunami and S. Kimura, Phys. Rev. B **84** (2011) 121411(R) .

BL7U

Inelastic Scattering of Photoelectrons at Organic/Graphite Interface

 T. Yamaguchi¹, F. Bussolotti², J. Yang¹, K. Kimura¹, M. Matsunami², N. Ueno¹ and S. Kera^{1,2}
¹Graduate School of Advanced Integration Science, Chiba University, Chiba 263-8522, Japan

²Institute for Molecular Science, Okazaki 444-8585, Japan

Understanding electron-phonon coupling as well as *weak* intermolecular interaction is required to discuss the mechanism of charge transport in functional molecular materials. The experimental study of electron-phonon coupling of the highest occupied molecular orbital (HOMO) state in the ordered monolayer film is essential to comprehend hole-hopping transport and small-polaron related transport [1]. In this work, we succeeded to observe a modulation of energy loss of photoelectron from graphite by exciting *intramolecular* vibration of adsorbed organic molecule at the substrate surface.

Low-energy excited angle-resolved ultraviolet photoelectron spectroscopy (ARUPS) was performed at beamline BL7U. A highly oriented pyrolytic graphite (HOPG) substrate was cleaned by heating at 900K for 2h. Pentacene (PEN) and zinc phthalocyanine (ZnPc) were deposited on the HOPG at < 0.1nm/min at room temperature, then the film was annealed to obtain the well-ordered monolayer.

First derivative of ARUPS intensity maps for PEN/HOPG and ZnPc/HOPG are shown in Fig.1 (a) and (b), respectively. Strong peaks beneath the Fermi level due to scattering from k-point of graphite (red arrows) are observed similarly to the previous report [2]. To exclude the impact of intensity background by the strong peaks, energy distribution curve, $I_0(E)$ was integrated for $\theta = 0 \pm 3^\circ$. In Fig. 2, photon energy dependence of $I_0(E)$ (top panel) and their derivatives, $-dI_0(E)/dE$ (bottom) taken for photon energies of 7~11eV are shown for PEN/HOPG.

Clearly one can find peaks observed strongly at $E_b=170$ meV for higher energy excitation and weakly at $E_b=90$ meV for lower energy excitation in Fig. 2(b). Tanaka *et al.*, reported ARUPS result of a bare HOPG where features of energy loss of photoelectron (60~70 and 154~175 meV) due to inelastic scattering by graphite phonon are observed with phonon dispersion [3]. Comparing to the bare surface, the loss energy increases from 154 meV to 170 meV and 67 meV to 90 meV at Γ point, respectively with no energy dispersion. Similar results are observed for ZnPc (not shown). The energy loss of 170 meV may correspond to the effective vibronic coupling mode of 167 meV for PEN/HOPG and 170 meV for ZnPc/HOPG detected for HOMO in high-resolution UPS [1]. We observed that the energy dependences of the intensity of both peaks are similar to that of the bare surface, indicating that the process of the inelastic scattering would be bounded by the resonance excitation channels of the graphite [3], however the frequency

of emitted phonon is arranged by exciting *intramolecular* vibrations. Obviously, the observed intensity is too large for *extrinsic* energy loss in propagation process to the surface as found for HREELS (on the order of 10^{-3}), indicating that the inelastic scattering could be dominated by *intrinsic* loss of photoelectron at molecule/graphite interface where the wavefunction of electron couples strongly to that of *intramolecular* vibrations.

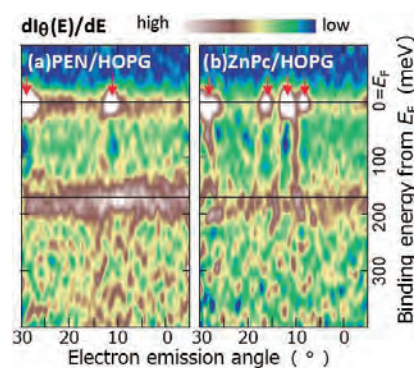


Fig. 1. First derivative of ARUPS intensity map taken at $h\nu=11$ eV for PEN/HOPG at 11 K (a) and ZnPc/HOPG at 14 K (b).

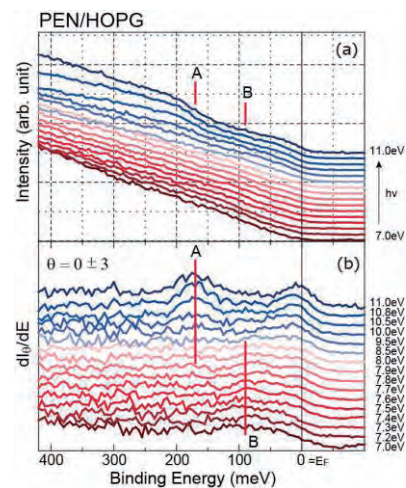


Fig. 2. Photon-energy dependence of $I_0(E)$ and $dI_0(E)/dE$ for PEN/HOPG ($\theta=0 \pm 3^\circ$).

- [1] S. Kera *et al.*, Prog. Surf. Sci. **84** (2009) 135.
- [2] H. Yamane *et al.*, UVSOR Activity Report 2013 **41** (2014) 144.
- [3] S. Tanaka *et al.*, Sci. Rep. **3** (2013) 3031.

BL8B

Direct Observation of Electronic Structure of Nylon-6,6 to Clarify the Contact Electrification Mechanism

T. Sato¹, K. R. Koswattage², Y. Nakayama¹ and H. Ishii^{1,2}

¹Graduate School of Advanced Integration Science, Chiba University, Chiba 263-8522, Japan

²Center for Frontier Science, Chiba University, Chiba 263-8522, Japan

Contact electrification of insulating polymers has been widely used in several technologies such as laser printing and photocopying. But the fundamental mechanism of this phenomenon is still controversial, and several models have been discussed [1]. In most models such as surface state model [2] and molecular-ion-state model [3], the existence of the some gap states is often assumed between highest occupied molecular orbital (HOMO) and lowest unoccupied molecular orbital (LUMO). These states can work as charge reservoir for the charge transfer upon the contact electrification. However, the direct observation of the electronic structure including gap states was examined only for very limited insulating polymers. Therefore, the investigation of the electronic structure of insulating polymers is important to clarify the contact electrification mechanism. In this study, the electronic structure of Nylon-6,6 including gap states was observed by not only ultraviolet photoemission spectroscopy (UPS) at BL8B of UVSOR but also high sensitivity UPS and photoelectron yield spectroscopy (PYS) at handmade apparatus of our laboratory [4].

Figure 1 shows the UPS spectrum of Nylon-6,6 thin film, which was made by spin coating on indium-tin oxide (ITO) substrate. The ionization energy (I) of Nylon-6,6 is determined as 7.49 eV from the onset of the photoemission from the HOMO. Moreover, the photoemission was detected from the vicinity of 4.3 eV by high sensitivity PYS. This result suggests that the gap states of Nylon-6,6 exist from the HOMO to at least 3.2 eV above, and the existence of such gap states was also confirmed by high sensitivity UPS by using pure deep UV light with extremely low stray light. These gap states are related to the charge transfer upon the contact electrification.

In PYS measurement, the information on the density of states (DOS) of the sample can be obtained in principle by differentiating the PYS spectrum with respect to photon energy [5]. Accordingly, we determined the DOS distribution of nylon-6,6 including gap states by combining the UPS at BL8B, high sensitivity UPS, and high sensitivity PYS results (Fig. 2). As a result, the density of states of gap states near the Fermi level of the substrate was about 10^{-5} times smaller than that of HOMO. Besides, using this observed DOS distribution, we estimated the charge density during the contact electrification if the charge transfer occurs via only gap states. Consequently, the order of estimated charge density was consistent with

that of the literature data observed by Kelvin Probe. This result suggests that contact electrification of insulating polymers can be explained by charge transfer via only gap states.

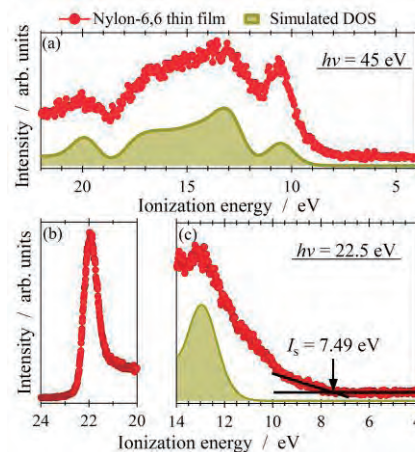


Fig. 1. (a) UPS spectrum of Nylon-6,6 thin film and a simulated density of states curve of Nylon-6,6 based on quantum chemical calculation (Gaussian09 with B3LYP/6-31g basis set). (b) UPS spectrum of the SECO region. (c) UPS spectrum of the top valence region.

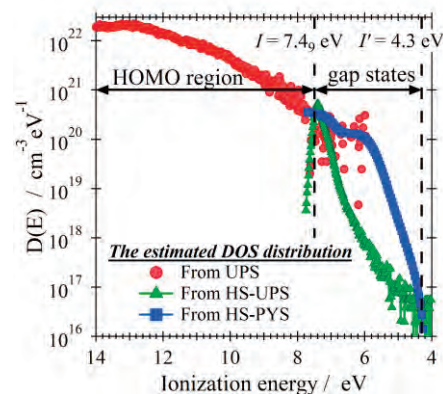


Fig. 2. The density of states of Nylon-6,6 estimated from UPS and PYS spectra.

[1] S. Matsusaka *et al.*, Chem. Eng. Sci. **65** (2010) 5781.

[2] J. Lowell, Adv. In Phys. **29** (1980) 947.

[3] C. B. Duke *et al.*, J. Appl. Phys. **49** (1978) 315

[4] S. Machida *et al.*, Appl. Phys. Express **6** (2013) 025801.

[5] J. Szuber, Vacuum **57** (2000) 209.

BL8B/BL2B

Investigation of Charge-Transfer Interaction by Metal Deposition on Organic Semiconducting Thin Films

T. Hosokai¹, K. Yonezawa², R. Makino², K. R. Koswattage², K. K. Okudaira² and S. Kera^{2,3}¹National Institute of Advanced Industrial Technology and Science, Tsukuba 305-8568, Japan²Graduate School of Advanced Integration Science, Chiba 263-8522, Japan³Department of Photo-Molecular Science, Institute for Molecular Science, Okazaki 444-8585, Japan

Understanding the impact of the electronic structure on the charge-transfer (CT) interaction between organic semiconductors and noble metals is highly important for *Organic Electronics*, because their interfacial energy-level alignment determines an efficiency of charge-carrier injection. Previously, we have proposed that such a CT can happen for organic-on-metal systems (as seen in Figs. 1(a) and 1(b) top) due to surface-induced aromatic stabilization (SIAS), and the SIAS takes place owing to a specific chemical structure of the adsorbates [1,2,3]. However, it is still not clear whether the SIAS can also occur for metal-on-organic systems, which is usually used in organic devices as a top-contact fabrication. Here, we investigated the electronic structure of a prototypical organic semiconductor, diindenoperylene (DIP: C₃₂H₁₆, Fig. 1(b)), thin films by using angle-resolved ultraviolet photoelectron spectroscopy (ARUPS).

All the experiments were conducted at BL8B in UVSOR. After preparing a clean SiO₂/Si wafer or Au-coated Si wafer, DIP films were thermally grown on the surfaces in situ with a nominal film thickness of 20 nm. There, DIP molecules orient with up-right standing on SiO₂ surface or lying-down on Au surface, which exhibit a large difference in energy of molecular features relative to the Fermi level (see the bottom spectrum in Figs. 1(a) and 1(b)). Then, Ag or Cu was thermally deposited step-by-step on those DIP films. ARUPS was measured at each deposition amount of the metals, with a photoelectron emission angle $\theta=40^\circ$ at $h\nu=28$ eV. All the depositions and measurements were performed at room temperature.

Figures 1(a) and 1(b) show the ARUPS results of Ag or Cu/DIP systems as a function of the metal deposition amount, where spectra of DIP monolayer/Ag or Cu polycrystalline (poly) surface systems are also depicted. The bottom spectrum of each DIP film clearly shows no gap states. As metals are deposited on the DIP films, abundant gap states immediately appear and grow together with a distinct feature colored by green, which is resembled to the DIP/Ag or DIP/Cu systems. These results imply that the observed distinct feature in the metal/DIP systems is caused by CT interaction between the deposited metals and DIP. Thus, it can be concluded that SIAS can occur even for a top-contact condition as the same as a bottom-contact condition, which should be a key to realize Ohmic contacts in various organic devices. Furthermore, the molecular orientations do not effect formation of the CT state.

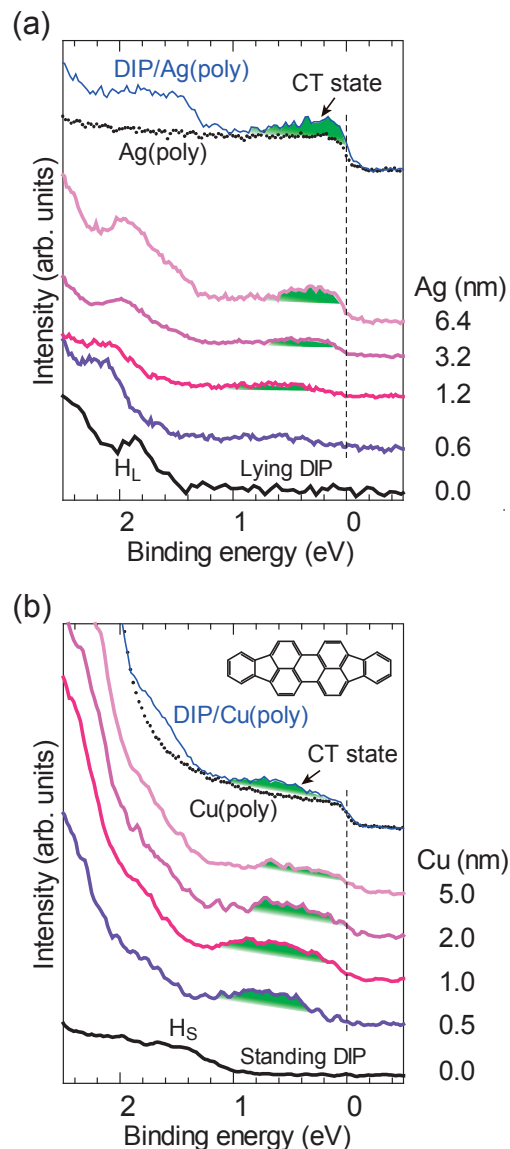


Fig. 1. ARUPS of Ag (a) and Cu (b) deposited on DIP (inset in (b)) thick films, where spectra of DIP monolayer on Ag(poly) or on Cu(poly) systems are also depicted. H_s and H_L indicates the highest occupied molecular orbital band of standing and lying DIP films.

[1] G. Heimel *et al.*, *Nature Chem.* **5** (2013) 187.[2] T. Hosokai *et al.*, *MRS proceedings 2013, 1647, mrsf13-1647-gg01-03.*[3] T. Hosokai *et al.*, *UVSOR Activity Report 2013* **41** (2014) 152.